

1 **Persistent Multi-Scale Consistency in Best-**
2 **Track Intensity Evolution and Rapid**
3 **Intensification in Atlantic Tropical Cyclones**
4 **(1851–2024)**

5 Nathan Howell
6 PTEM Labs, Atlantic Beach, Florida, USA
7 ORCID: 0009-0009-8893-6260
8 Email: nate@ptemplabs.com

9 **Preprint statement:**

10 This manuscript is a non-peer reviewed preprint submitted to EarthArXiv. A version of this work
11 has been submitted to *Weather and Forecasting* (WAF) for peer review.

12
13
14
15
16
17
18
19
20
21
22
23
24
25
26
27
28
29
30
31
32
33
34
35
36
37
38

39 **Persistent Multi-Scale Consistency in Best-**
40 **Track Intensity Evolution and Rapid**
41 **Intensification in Atlantic Tropical Cyclones**
42 **(1851–2024)**

43 **Nathan Howell**
44 PTEM Labs, Atlantic Beach, Florida, USA
45 ORCID: 0009-0009-8893-6260

46 Corresponding author: nate@ptemplabs.com

47

48 **Abstract**

49 Rapid intensification (RI), commonly defined as an increase in maximum sustained wind speed
50 of at least 30 kt within 24 h, remains one of the most challenging aspects of tropical cyclone
51 forecasting.

52 This study evaluates whether persistent multi-scale consistency in best-track intensity evolution
53 is statistically associated with RI occurrence across the full Atlantic historical record. A minimal,
54 forward-only diagnostic is constructed from HURDAT2 using causal rolling means of maximum
55 sustained wind speed at multiple timescales and a directional-agreement rule across scales. The
56 method uses only current and prior best-track intensity values and is applied uniformly to 1,991
57 Atlantic tropical cyclones from 1851 to 2024.

58 Storms exhibiting longer durations of persistent multi-scale agreement form a small subset with
59 substantially elevated RI occurrence. As persistence increases, RI probability rises from a basin-
60 wide baseline of approximately 26% to about 60% for storms with at least 140 h of persistence
61 and to about 67% for storms with at least 168–270 h of persistence.

62 The diagnostic is not interpreted as a direct measure of inner-core structure and is not proposed
63 as an operational forecast tool. Instead, it provides a reproducible long-record statistical
64 diagnostic derived solely from best-track data. The results indicate that prolonged multi-scale
65 consistency identifies a subset of storms with substantially elevated RI likelihood and motivate
66 further comparison with higher-resolution structural observations.

67

68 **1. Introduction**

69 Rapid intensification (RI), typically defined as an increase in maximum sustained wind speed of
70 at least 30 kt within 24 h, remains one of the most consequential and difficult-to-forecast aspects
71 of tropical cyclone evolution (Kaplan and DeMaria 2003; Kaplan et al. 2010; DeMaria et al.
72 2021). Despite advances in statistical-dynamical guidance and environmental diagnostics, RI
73 continues to exhibit substantial variability, with storms in similar large-scale environments often
74 evolving differently.

75 Previous work has emphasized the role of environmental conditions such as vertical wind shear,
76 sea surface temperature, and ocean heat content (Kaplan and DeMaria 2003; Kaplan et al. 2010).
77 At the same time, a growing body of observational and modeling research highlights the
78 importance of internal storm structure, including convective symmetry, vortex alignment, and
79 inner-core evolution (Jiang 2012; Kieper and Jiang 2012; Rogers et al. 2015; Miyamoto and
80 Nolan 2018; Shi et al. 2023). These results suggest that RI is influenced by both environmental
81 forcing and evolving storm organization.

82 However, structurally informative observations are largely confined to the satellite and aircraft
83 reconnaissance eras. In contrast, the Atlantic best-track dataset (HURDAT2) provides basin-wide
84 coverage extending back to the mid-nineteenth century but contains limited direct information
85 about storm structure (Landsea and Franklin 2013; Landsea et al. 2022; Vecchi and Knutson
86 2008, 2011).

87 This disparity motivates a simpler question: does the time evolution of best-track intensity
88 contain a persistent statistical relationship associated with RI? Specifically, can a minimal,
89 forward-only diagnostic derived solely from best-track intensity identify a subset of storms with
90 systematically elevated RI likelihood?

91 The present study addresses this question using the full Atlantic record from 1851 to 2024. A
92 persistence diagnostic is constructed using multi-scale smoothing and directional agreement
93 applied to intensity evolution. The method is intentionally minimal and designed for consistent
94 application across the full historical archive.

95 The objective is not to develop an operational prediction system or to directly diagnose inner-
96 core structure. Instead, the study evaluates whether prolonged multi-scale consistency in
97 intensity evolution identifies a statistically distinct subset of storms with elevated RI occurrence.
98 If such a relationship exists, it would provide a long-record statistical perspective complementary
99 to modern structural diagnostics.

100
101 A companion analysis applying identical construction to the Eastern Pacific basin is presented
102 separately.

103

104

105 2. Data

106 This analysis uses the Atlantic hurricane database HURDAT2 (Landsea et al. 2022), which
107 contains best-track information for 1,991 tropical cyclones spanning 1851–2024 at a 6-h
108 advisory interval. For each storm and advisory time, the dataset provides storm position and
109 maximum sustained wind speed (VMAX). In this study, VMAX is used to construct the
110 persistence diagnostic and to define RI events.

111 Rapid intensification is defined as an increase in VMAX of at least 30 kt over 24 h, consistent
112 with established operational and research conventions (Kaplan and DeMaria 2003; Kaplan et al.
113 2010; DeMaria et al. 2021).

114 HURDAT2 is not temporally homogeneous across the full record. Earlier portions of the dataset
115 are subject to greater uncertainty in storm detection and intensity estimation, particularly prior to
116 the satellite era (Landsea and Franklin 2013; Vecchi and Knutson 2008, 2011; Vecchi et al.
117 2021). These limitations are considered in interpretation but are not explicitly corrected in the
118 present analysis. The goal is to evaluate whether a simple within-storm persistence property is
119 associated with RI across the archive despite these known constraints.

120

121 3. Methods

122 3.1. Persistence diagnostic

123 Let ($V(t)$) denote maximum sustained wind speed at 6-h intervals. To characterize intensity
124 evolution across multiple temporal scales, three causal rolling means are computed:

$$\begin{aligned} 125 & [\\ 126 & V_3(t), \quad V_5(t), \quad V_9(t) \\ 127 &] \end{aligned}$$

128 where each rolling mean is calculated using only the current and preceding observations.

129 For each smoothed series, a one-step tendency is defined as:

$$\begin{aligned} 130 & [\\ 131 & D_s(t) = V_s(t) - V_s(t-1), \quad s \in \{3,5,9\}. \\ 132 &] \end{aligned}$$

133 Directional agreement is evaluated across three window pairs: ((3,5)), ((5,9)), and ((3,9)). For
134 each pair, define:

135 [

136 $A_{ij}(t) =$

137 \begin{cases}

138 $1, & \text{if } \mathrm{sign}(D_i(t)) = \mathrm{sign}(D_j(t)) \setminus$

139 $0, & \text{otherwise}.$

140 \end{cases}

141]

142 The multi-scale agreement score is:

143 [

144 $PL(t) = \frac{1}{3} \sum A_{ij}(t),$

145]

146 which ranges from 0 to 1 and measures directional consistency across temporal scales.

147

148 **3.2. Activation rule and persistence**

149 A time step is classified as active when:

- 150
- ($PL(t) \geq 0.67$), and
 - 151 • the condition persists for at least two consecutive advisories.

152 This requirement ensures that activation reflects sustained rather than transient agreement.

153 For each storm, persistence is defined as:

154 [

155 $\text{Persistence} = N_{\text{active}} \times 6 \text{ h},$

156]

157 where (N_{active}) is the number of active time steps. Persistence therefore represents

158 the total duration of sustained multi-scale agreement in intensity evolution.

159 All statistics are computed at the storm level to avoid temporal dependence within individual

160 storm time series.

161

162 **3.3. Interpretation**

163 The persistence diagnostic is intended as a minimal proxy for sustained multi-scale consistency

164 in best-track intensity evolution. It is not a direct measurement of inner-core structure and does

165 not incorporate environmental predictors. Its purpose is to determine whether prolonged multi-

166 scale agreement in intensity tendency identifies a statistically distinct subset of storms within the
167 historical record. The use of multi-scale smoothing and directional agreement is conceptually
168 consistent with prior applications of scale-dependent coherence in geophysical time series
169 (Torrence and Compo 1998; Grinsted et al. 2004; Ng and Chan 2012).

170
171

172 **3.4. Comparison metric: single-scale persistence**

173

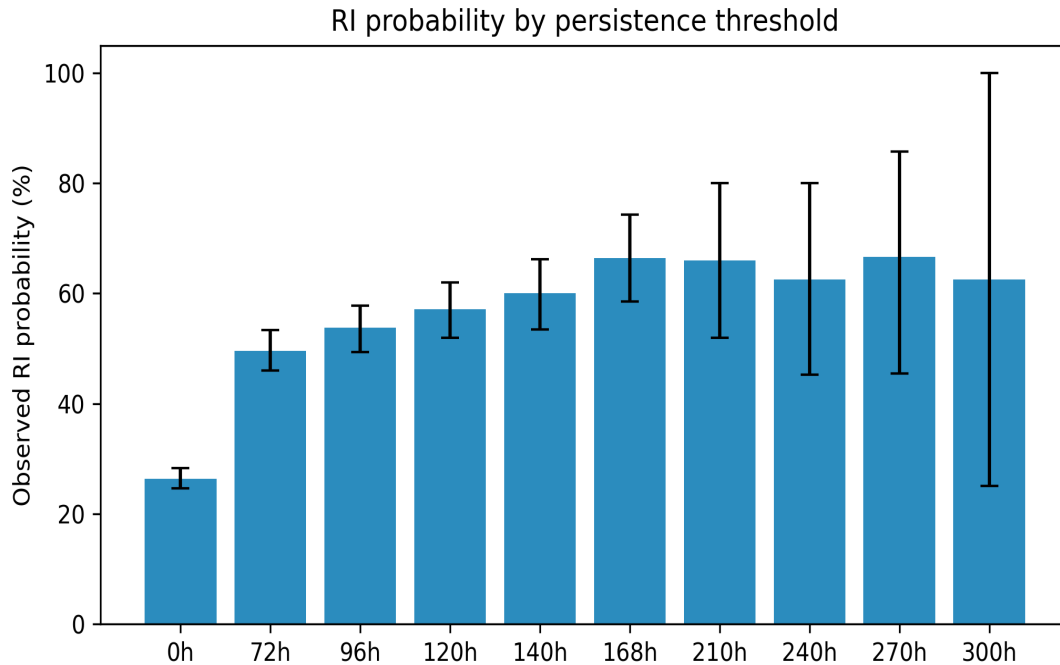
174 To assess whether the multi-scale persistence diagnostic adds information beyond simpler
175 persistence measures, a single-scale comparison metric was also constructed. This comparison
176 metric uses only the 5-step causal rolling mean of VMAX, with activity defined when the one-
177 step tendency remains positive for at least two consecutive advisories. Storm-level persistence is
178 then defined as the total duration of active time steps, using the same 6-h accumulation rule
179 applied to the multi-scale diagnostic. This comparison is intended to isolate the contribution of
180 cross-scale agreement relative to a simpler single-scale persistence measure.

181

182 **4. Results**

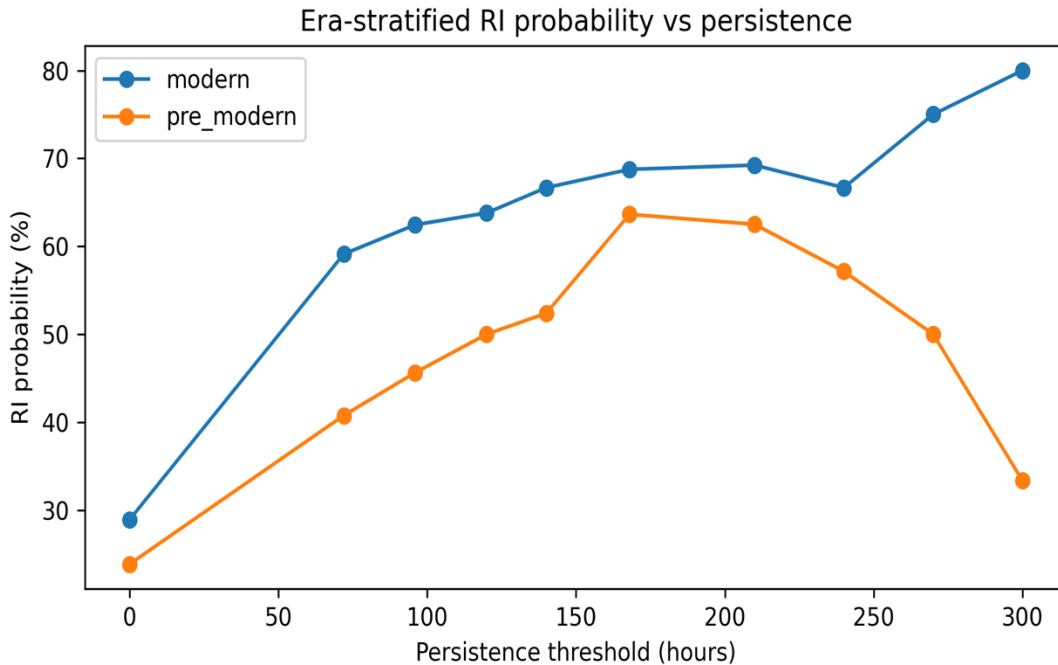
183 Across the Atlantic dataset (1851–2024; 1,991 storms), 525 storms satisfy the rapid
184 intensification (RI) definition, corresponding to a basin-wide RI probability of approximately
185 26.4%.

186 Storms stratified by persistence duration exhibit a clear and largely monotonic increase in RI
187 probability (Fig. 1). For storms with persistence of at least 72 h, the RI probability increases to
188 approximately 49.6% ($n = 659$). At higher persistence thresholds, the enrichment continues:
189 60.1% for ≥ 140 h ($n = 228$), 66.4% for ≥ 168 h ($n = 146$), and 66.7% for ≥ 270 h ($n = 24$). These
190 values correspond to a roughly 2.3–2.5 \times increase relative to the basin baseline (26.4%).



191 Fig. 1. RI probability as a function of persistence duration threshold. Error
 192 bars indicate bootstrap confidence intervals. Sample sizes decrease with
 193 increasing threshold, leading to wider uncertainty beyond ~168 h. Sample
 194 sizes decrease from $n = 1991$ at 0 h to $n = 24$ at 270 h and $n = 8$ at 300 h.
 195

196
 197 Stratification by observational era shows that the persistence–RI relationship is preserved across
 198 multiple historical regimes (Fig. 3), with similar monotonic structure evident in pre-1944, mid-
 199 century, and modern subsets. Differences in absolute RI probability across eras are consistent
 200 with known observational and intensity estimation differences, but the underlying relationship
 201 remains intact.
 202
 203



204

205 Fig. 3. RI probability as a function of persistence duration stratified by
 206 observational era (pre-modern vs modern). Both subsets exhibit similar
 207 monotonic enrichment, indicating that the persistence-RI relationship is not
 208 dependent on the observing system.

209

210 Bootstrap confidence intervals indicate that the enrichment remains statistically distinct from the
 211 baseline across thresholds up to at least 168 h (e.g., 0.534–0.662 at 140 h; 0.585–0.744 at 168 h).
 212 At higher thresholds, confidence intervals widen due to decreasing sample size, but point
 213 estimates remain elevated.

214 The persistence diagnostic therefore identifies a conditionally enriched subset rather than
 215 providing broad detection of all RI events. The observed pattern is best interpreted as evidence
 216 that prolonged multi-scale consistency in intensity evolution is associated with a distinct class of
 217 storm behavior within the historical record.

218

219 5. Robustness and Sensitivity Analyses

220 5.1. Bootstrap uncertainty

221 Uncertainty in the persistence-RI relationship was evaluated using storm-level bootstrap
 222 resampling. Across all persistence thresholds, bootstrap confidence intervals remain well above

223 the basin baseline, indicating that the observed enrichment is not driven by sampling variability.
224 While uncertainty increases in the highest-persistence cohorts due to small sample size, the
225 central tendency of the relationship remains stable.

226

227 **5.2. Permutation null test**

228 To assess whether the observed enrichment could arise from random association between
229 persistence and RI, a permutation null test was conducted in which RI labels were randomly
230 reassigned across storms. Under this null hypothesis, the persistence–RI relationship collapses,
231 and the probability of observing enrichment comparable to the empirical result is low ($p < 0.01$
232 across thresholds).

233 This indicates that the observed monotonic increase in RI probability with persistence duration is
234 not consistent with random assignment and reflects a structured relationship within the dataset.

235

236 **5.3. Block-shuffle null**

237 A more stringent null was constructed by applying block-wise temporal shuffling within storms,
238 which disrupts temporal multi-scale consistency in intensity evolution while preserving marginal
239 intensity distributions and coarse storm structure.

240 Under this null, partial overlap with the observed statistical relationship is present at some
241 thresholds, indicating that aspects of the persistence–RI relationship are embedded in the
242 temporal evolution of intensity itself. This result supports the interpretation that persistence
243 captures meaningful properties of intensity evolution rather than representing a fully independent
244 structural association.

245

246 **5.4. Sensitivity to parameter choices**

247 The persistence–RI relationship was evaluated under multiple parameter configurations,
248 including alternate smoothing windows and stricter activation rules. Across these configurations,
249 the monotonic enrichment pattern is preserved, and effect sizes remain similar to the baseline
250 configuration.

251 This indicates that the result is not dependent on a specific parameter choice and is robust to
252 reasonable variations in construction.

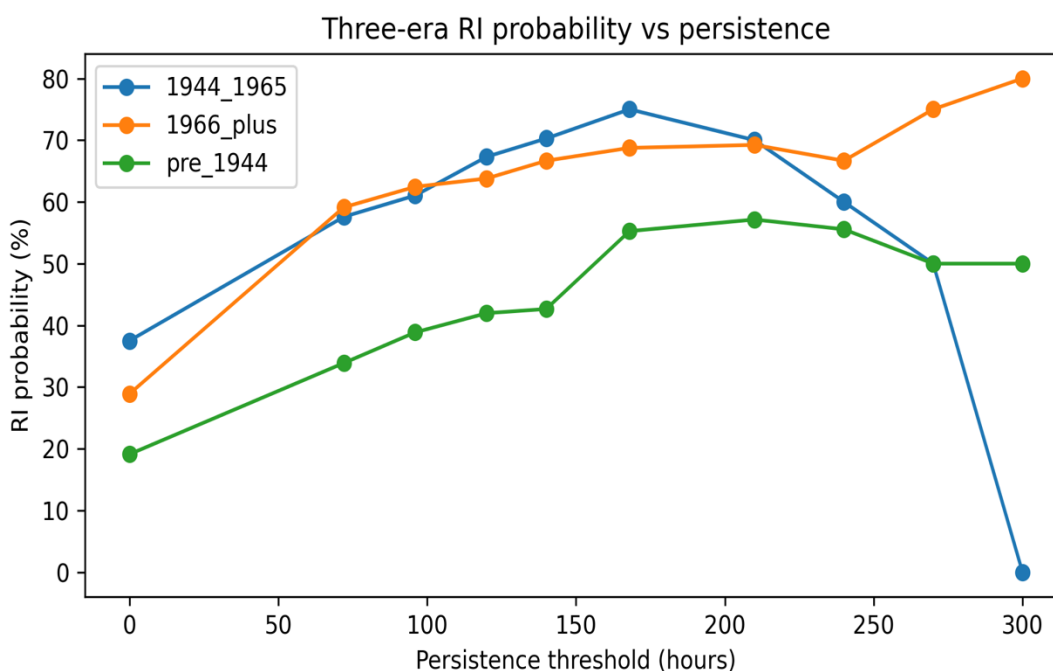
253

254 5.5. Observational era stratification

255 The dataset was partitioned into pre-modern and modern observational eras. In both subsets, the
256 persistence–RI relationship is preserved. RI probability increases from approximately 24% to
257 approximately 63% in the pre-modern subset and from approximately 29% to approximately
258 69% in the modern subset at comparable persistence thresholds.

259 The persistence–RI relationship remains consistent across all three observational eras (Fig. 4),
260 with similar monotonic structure despite differences in absolute probability levels.

261
262



263

264 Fig. 4. RI probability as a function of persistence duration across three observational eras. All subsets exhibit similar
265 monotonic structure, with differences in magnitude consistent with known observational and intensity estimation
266 differences. The preservation of the relationship across eras indicates that the persistence–RI association is robust to
267 historical inhomogeneities in the best-track record. Estimates at the highest thresholds are based on small sample
268 sizes and should be interpreted cautiously.

269

270 5.6. Duration normalization

271 To evaluate whether persistence simply reflects storm duration, a duration-normalized
272 persistence metric was analyzed. The persistence–RI relationship remains monotonic under
273 normalization, indicating that persistence captures additional information beyond storm lifetime.

274

275 **5.7. Pre-event persistence**

276 Persistence computed prior to RI onset is rare at high thresholds and associated with small
277 sample sizes. While estimates are therefore uncertain, the presence of elevated persistence prior
278 to RI onset suggests that sustained temporal multi-scale consistency can precede intensification
279 events. These results should be interpreted cautiously.

280

281 **5.8. Logistic regression analysis**

282 Logistic regression models were constructed to evaluate whether persistence provides
283 independent explanatory information beyond storm duration.

284 In a univariate model, persistence exhibits a positive and statistically significant coefficient ($\beta \approx$
285 0.015 h^{-1} ; odds ratio ≈ 1.015 per hour). When storm duration is included as a covariate, the
286 persistence coefficient remains unchanged, while the duration coefficient collapses toward zero.

287 This indicates that the persistence–RI relationship is not reducible to storm lifetime and that
288 persistence provides independent explanatory statistical association beyond storm duration.

289

290

291 **5.9. Comparison with a single-scale persistence metric**

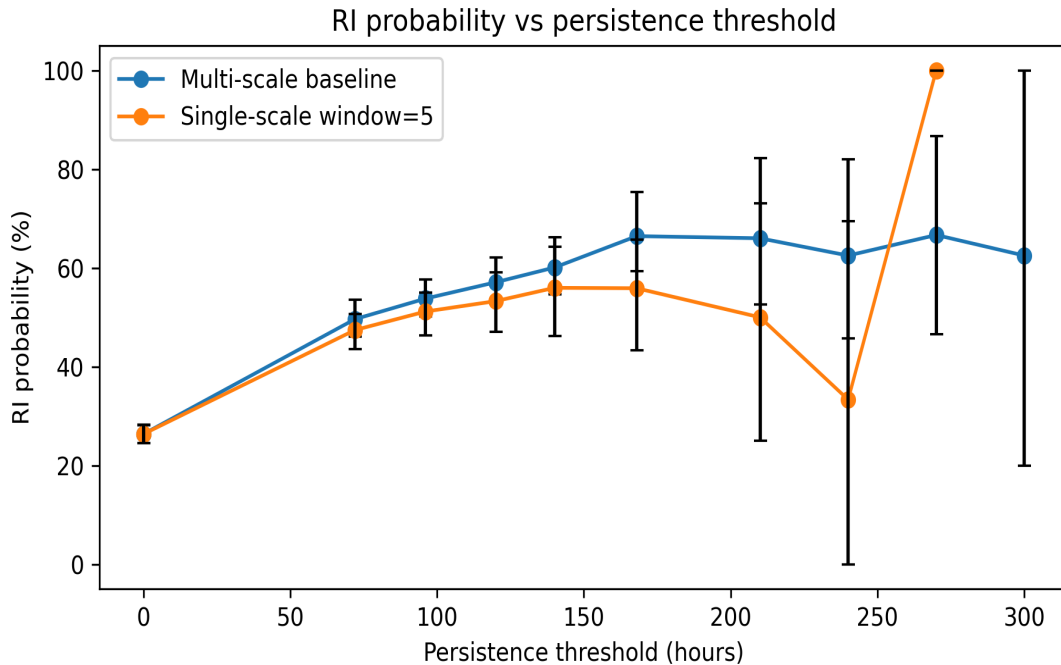
292

293 To evaluate whether the observed relationship depends on the multi-scale construction, a
294 comparison was performed using a single-scale persistence metric.

295 The single-scale comparator also exhibits increasing RI probability with persistence duration,
296 indicating that persistence in intensity evolution itself contains meaningful association. However,
297 the multi-scale diagnostic yields systematically stronger and more stable enrichment across
298 thresholds. For example, RI probability increases to approximately 66% at ≥ 168 h for the multi-
299 scale diagnostic, compared to approximately 56% for the single-scale comparator.

300

301



302 Fig. 2. Comparison of multi-scale persistence diagnostic and single-scale
 303 persistence metric. While both exhibit increasing RI probability with
 304 persistence, the multi-scale diagnostic produces stronger and more stable
 305 enrichment across thresholds, particularly at intermediate durations (72-168
 306 h).
 307
 308

309
 310 At higher persistence thresholds, the single-scale comparator becomes unstable due to small
 311 sample sizes, with sharp fluctuations in estimated RI probability. In contrast, the multi-scale
 312 diagnostic maintains a more consistent upper-tail behavior, indicating improved discrimination
 313 of persistent storm evolution.

314 Logistic regression results further support this distinction. While single-scale persistence is
 315 positively associated with RI occurrence, its effect weakens when controlling for storm duration.
 316 In contrast, the multi-scale persistence metric retains a stronger and more stable relationship with
 317 RI under duration control, indicating that it captures additional structure beyond simple storm
 318 longevity.

319 These results indicate that persistence in intensity evolution contains meaningful information, but
 320 that requiring directional agreement across multiple temporal scales sharpens the identification
 321 of storms with elevated RI likelihood. This isolates the contribution of cross-scale agreement
 322 while holding persistence definition constant.

324

6. Discussion

325 The principal result of this study is that prolonged multi-scale consistency in best-track intensity
326 evolution is associated with a conditionally enriched subset of storms exhibiting elevated RI
327 occurrence across the Atlantic historical record. This relationship is supported by monotonic
328 enrichment across persistence thresholds, robustness to parameter variation, and independence
329 from storm duration in regression analysis.

330 Comparison with a single-scale persistence metric indicates that persistence in intensity
331 evolution itself contains meaningful association, but that requiring directional agreement across
332 multiple temporal scales yields stronger and more stable separation of high-RI subsets. In
333 particular, the multi-scale diagnostic produces consistently higher RI probabilities across
334 intermediate thresholds (72–168 h) and maintains more stable behavior in the upper tail, where
335 the single-scale comparator becomes sensitive to small sample sizes. This suggests that cross-
336 scale agreement provides additional structure beyond persistence at a single smoothing scale.

337 The persistence–RI relationship is preserved across observational eras, with similar monotonic
338 behavior evident in pre-1944, mid-century, and modern subsets. Differences in absolute RI
339 probability across eras are consistent with known changes in observational coverage and
340 intensity estimation, but the underlying relationship remains intact. This indicates that the
341 statistical relationship is not an artifact of the observing system and reflects a persistent property
342 of storm evolution captured in the best-track record.

343 These findings are consistent with prior observational and modeling studies linking RI to
344 evolving storm organization, including convective symmetry, precipitation structure, and vortex
345 alignment (Jiang 2012; Rogers et al. 2015; Miyamoto and Nolan 2018; Shi et al. 2023). The
346 present analysis does not resolve these processes directly, but demonstrates that a simple
347 diagnostic derived from intensity evolution alone is associated with systematically different RI
348 likelihood.

349 The persistence diagnostic differs fundamentally from the RI definition itself. RI is defined by a
350 fixed magnitude threshold over a specified time interval (Kaplan and DeMaria 2003), whereas
351 the persistence metric reflects sustained directional agreement across multiple temporal scales.
352 The presence of high-persistence storms that do not undergo RI indicates that the diagnostic
353 captures a broader property of storm evolution rather than a direct transformation of intensity
354 change.

355 Attenuation under block shuffling indicates dependence on temporal ordering, consistent with
356 the diagnostic capturing structured evolution rather than marginal intensity properties alone. This
357 is consistent with the interpretation that persistence reflects sustained multi-scale consistency in
358 intensity evolution, rather than a fully independent structural variable.

359

360 The persistence diagnostic presented here is derived entirely from best-track intensity evolution
361 and therefore is not independent of the underlying intensity signal used to define rapid
362 intensification (RI). However, it differs fundamentally from magnitude-based RI definitions in

363 that it does not depend on threshold exceedance over a fixed time interval, but instead reflects
364 sustained directional consistency across multiple temporal scales. The comparison with a single-
365 scale persistence metric further indicates that persistence alone does not fully account for the
366 observed relationship; requiring agreement across temporal scales yields stronger and more
367 stable enrichment of RI probability. The persistence diagnostic should therefore be interpreted as
368 identifying a statistical regime within storm evolution rather than as a direct proxy for physical
369 structure or a predictive model of intensification.

370 At the same time, uncertainties in the historical best-track record, particularly prior to the
371 satellite era, may influence both persistence estimates and RI classification. The preservation of
372 the persistence–RI relationship across observational eras indicates that the signal is not solely an
373 artifact of changing observing systems, but the results should nevertheless be interpreted as a
374 long-record statistical association rather than a direct measurement of underlying physical
375 processes.

376 Taken together, these results indicate that persistent multi-scale consistency in intensity
377 evolution identifies a statistically distinct subset of storms with elevated RI likelihood, using
378 only best-track data and without reliance on environmental predictors or satellite-era structural
379 diagnostics.

380

381 **7. Limitations**

382 Several limitations should be noted:

- 383 • The highest-persistence subsets contain relatively few storms, limiting statistical
384 precision.
- 385 • The diagnostic is derived solely from best-track intensity and does not directly measure
386 physical storm structure.
- 387 • The analysis is observational and does not establish causality.
- 388 • HURDAT2 contains known inhomogeneities across observing eras.
- 389 • While multiple robustness analyses are included, additional work could further evaluate
390 alternative definitions, basin extensions, and physical interpretation.

391

392 **8. Conclusion**

393 A forward-only persistence diagnostic derived from best-track intensity evolution identifies a
394 small subset of Atlantic tropical cyclones with substantially elevated RI occurrence over 1851–
395 2024. This relationship is robust to bootstrap resampling, null testing, parameter variation, and
396 observational-era stratification and is not explained by storm duration alone.

397 The results demonstrate that persistent multi-scale consistency in intensity evolution is a
398 measurable and statistically stable property of storms in the historical record. This provides a
399 foundation for future work linking long-record intensity-based diagnostics with higher-resolution
400 structural observations.

401
402 Replication under identical construction in an independent basin further supports the
403 interpretation that this relationship reflects a general property of tropical cyclone intensity
404 evolution rather than a basin-specific artifact.

405

406 **9. Data Availability**

407 The Atlantic hurricane database (HURDAT2) used in this study is publicly available from the
408 National Hurricane Center (<https://www.nhc.noaa.gov/data/>). Code and derived data supporting
409 the persistence diagnostic are archived at Zenodo (DOI:
410 <https://doi.org/10.5281/zenodo.19273323>). The repository includes a minimal, reproducible
411 implementation of the diagnostic and example datasets sufficient to reproduce the analysis from
412 HURDAT2.

413

414

415 **10. Acknowledgements**

416 The author thanks the developers and maintainers of the HURDAT2 dataset and the broader
417 tropical cyclone research community for maintaining the historical record used in this analysis.

418 Large language models were used for editorial assistance and language refinement during
419 manuscript preparation. All scientific content, analysis, and interpretation are the responsibility
420 of the author.

421 This work received no external funding.

422 The author declares no conflicts of interest.

423

424 **11. References**

425 DeMaria, M., Franklin, J. L., Onderlinde, M. J., and Kaplan, J., 2021: Operational forecasting of
426 tropical cyclone rapid intensification at the National Hurricane Center. *Atmosphere*, **12**, 683.
427 <https://doi.org/10.3390/atmos12060683>

428 Grinsted, A., Moore, J. C., and Jevrejeva, S., 2004: Application of the cross wavelet transform
429 and wavelet coherence to geophysical time series. *Nonlinear Processes in Geophysics*, **11**, 561–
430 566. <https://doi.org/10.5194/npg-11-561-2004>

431 Jiang, H., 2012: The relationship between tropical cyclone intensity change and the strength of
432 inner-core convection. *Monthly Weather Review*, **140**, 1164–1176.
433 <https://doi.org/10.1175/MWR-D-11-00134.1>

434 Jiang, H., and Ramirez, E. M., 2013: Necessary conditions for tropical cyclone rapid
435 intensification as derived from 11 years of TRMM data. *Journal of Climate*, **26**, 6459–6470.
436 <https://doi.org/10.1175/JCLI-D-12-00432.1>

437 Kaplan, J., and DeMaria, M., 2003: Large-scale characteristics of rapidly intensifying tropical
438 cyclones in the North Atlantic basin. *Weather and Forecasting*, **18**, 1093–1108.
439 [https://doi.org/10.1175/1520-0434\(2003\)018<1093:LCORIT>2.0.CO;2](https://doi.org/10.1175/1520-0434(2003)018<1093:LCORIT>2.0.CO;2)

440 Kaplan, J., DeMaria, M., and Knaff, J. A., 2010: A revised tropical cyclone rapid intensification
441 index for the Atlantic and eastern North Pacific basins. *Weather and Forecasting*, **25**, 220–241.
442 <https://doi.org/10.1175/2009WAF2222280.1>

443 Kieper, M. E., and Jiang, H., 2012: Predicting tropical cyclone rapid intensification using the 37-
444 GHz ring pattern identified from passive microwave measurements. *Geophysical Research*
445 *Letters*, **39**, L13804. <https://doi.org/10.1029/2012GL052115>

446 Landsea, C. W., and Franklin, J. L., 2013: Atlantic hurricane database uncertainty and
447 presentation of a new database format. *Monthly Weather Review*, **141**, 3576–3592.
448 <https://doi.org/10.1175/MWR-D-12-00254.1>

449 Landsea, C. W., Franklin, J. L., and Beven, J. L., II, 2022: The revised Atlantic hurricane
450 database (HURDAT2): Documentation and format updates. National Hurricane Center, NOAA.
451 <https://www.nhc.noaa.gov/data/>

452 Miyamoto, Y., and Nolan, D. S., 2018: Structural changes preceding rapid intensification in
453 tropical cyclones as shown in a large ensemble of idealized simulations. *Journal of the*
454 *Atmospheric Sciences*, **75**, 555–569. <https://doi.org/10.1175/JAS-D-17-0177.1>

455 Ng, E. K. W., and Chan, J. C. L., 2012: Geophysical applications of partial wavelet coherence
456 and multiple wavelet coherence. *Journal of Atmospheric and Oceanic Technology*, **29**, 1845–
457 1853. <https://doi.org/10.1175/JTECH-D-12-00056.1>

458 Rogers, R. F., Reasor, P. D., and Zhang, J. A., 2015: Multiscale structure and evolution of
459 Hurricane Earl (2010) during rapid intensification as sampled by aircraft. *Monthly Weather*
460 *Review*, **143**, 536–562. <https://doi.org/10.1175/MWR-D-14-00175.1>

- 461 Shi, D., Chen, G., and Xie, X., 2023: Revisiting the relationship between tropical cyclone rapid
462 intensification and the distribution of inner-core precipitation. *Geophysical Research Letters*, **50**,
463 e2023GL104810. <https://doi.org/10.1029/2023GL104810>
- 464 Torrence, C., and Compo, G. P., 1998: A practical guide to wavelet analysis. *Bulletin of the*
465 *American Meteorological Society*, **79**, 61–78. [https://doi.org/10.1175/1520-](https://doi.org/10.1175/1520-0477(1998)079<0061:APGTWA>2.0.CO;2)
466 [0477\(1998\)079<0061:APGTWA>2.0.CO;2](https://doi.org/10.1175/1520-0477(1998)079<0061:APGTWA>2.0.CO;2)
- 467 Vecchi, G. A., and Knutson, T. R., 2008: On estimates of historical North Atlantic tropical
468 cyclone activity. *Journal of Climate*, **21**, 3580–3600. <https://doi.org/10.1175/2008JCLI2178.1>
- 469 Vecchi, G. A., and Knutson, T. R., 2011: Estimating annual numbers of Atlantic hurricanes
470 missing from the HURDAT database (1878–1965) using ship track density. *Journal of Climate*,
471 **24**, 1736–1746. <https://doi.org/10.1175/2010JCLI3810.1>
- 472 Vecchi, G. A., Delworth, T., Gudgel, R., Kapnick, S., Rosati, A., Wittenberg, A., Zeng, F.,
473 Anderson, W., Balaji, V., Dixon, K., et al., 2021: Tropical cyclone sensitivities to CO₂ doubling:
474 Roles of atmospheric resolution, synoptic variability, and background climate changes. *Climate*
475 *Dynamics*, **57**, 1965–1986. <https://doi.org/10.1007/s00382-021-05867-2>